CMS Physics Analysis Summary

Contact: cms-future-conveners@cern.ch 2013/10/09

Study of the Discovery Reach in Searches for Supersymmetry at CMS with 3000 fb^{-1}

The CMS Collaboration

Abstract

It is planned that the Large Hadron Collider will deliver an integrated luminosity of up to 3000 fb^{-1} for each experiment, requiring an upgrade of the detector which would otherwise not survive the radiation damage. The reach of several representative searches for supersymmetry with the upgraded detector is studied for this scenario, where a very high instantaneous luminosity will lead to a large number of pileup events in each bunch crossing. The studies comprise the production of gluinos decaying to third generation squarks as well as to light squarks, and the direct production of neutralino-chargino pairs decaying to final states including a Z and a W boson. Depending on the SUSY particles, we can improve the discovery reach by about 300 to 400 GeV increasing the luminosity from 300 to 3000 fb^{-1}. In addition, the possible gain from extending the tracker up to a pseudorapidity of four is studied for vector boson fusion processes.

1 Introduction

Despite the remarkable success of the standard model (SM), there are fundamental omissions in the theory to describe dark matter (DM) and the low and stable mass scale of the electroweak vacuum. Supersymmetry (SUSY) is still considered to be one of the most appealing extensions, most notably due to the fact that it provides a natural mechanism to cancel the quadratic divergences that appear in the Higgs mass – the well known "hierarchy problem". A natural solution to the hierarchy problem is provided by SUSY with relatively light third-generation squarks and gluinos [1, 2].

Dark matter constitutes nearly 80% of the matter of the universe and is strongly believed to be a particle in nature based on cosmological models and astrophysical data [3, 4]. Within the context of R-parity conserving SUSY, the lightest supersymmetric particle (LSP) is a viable DM candidate. In many models the LSP is the lightest neutralino ($\tilde{\chi}_1^0$), a mixture of Bino, Wino, and Higgsino states. Even if the colored sparticles are heavy, the electroweak sector is still expected to be light in many SUSY scenarios. In such a case neutralinos and charginos can be produced directly in electroweak processes, and also in vector boson fusion (VBF) [5, 6].

As the SUSY production cross sections for high-mass colored sparticles as well as for electroweak and VBF production are very low, it is important to collect as much data as possible at highest energies. Therefore, we investigate here the discovery reach for several representative SUSY searches for the expected luminosity of $3000\,\text{fb}^{-1}$. Such a high integrated luminosity exceeds the initial design value for CMS by a factor of ten and can only be reached after a second ("Phase II") upgrade of the Compact Muon Solenoid (CMS) experiment at the Large Hadron Collider (LHC) running at a center-of-mass energy of 14 TeV. Without a second upgrade, the inner and forward parts of the detector would suffer seriously due to radiation damage and are expected to become inoperable after the integrated luminosity of about $500\,\text{fb}^{-1}$. We also quote the discovery reach of the discussed SUSY analyses for the design integrated luminosity of $300\,\text{fb}^{-1}$ expected by the end of 2021.

The upgrade options that are currently under discussion include a scenario with a tracking detector which is extended into the forward region, up to a pseudorapidity of $|\eta| < 4$, where η is defined as $\eta = -\ln[\tan(\theta/2)]$, with θ being the polar angle of the trajectory of a particle with respect to the z axis. As SUSY particles are typically produced in the central region, we expect a gain in the signal-to-background ratio due to better identification of background processes, which tend to populate also the forward parts of the detector. Therefore, a degraded region in the forward region would significantly increase the backgrounds for SUSY searches. Especially in the VBF production case, the extended tracking is necessary to identify vertices and charged particle association to forward jets as a primary tool to remove pileup. For neutrals in the forward region, one of the most powerful pileup jet rejection methods is based on the shapes that occur from random jet overlaps - here the tracking will provide clean evaluation of the jet directions and lateral profiles to allow for algorithmic reduction of neutral backgrounds in the calorimeter.

In order to be as general as possible, we investigate simplified models [7–9] which are developed based on signal topology. This choice avoids the need of assuming a full model, with many fixed parameters and assumptions, which might lead to very specific signatures and is likely not to be representative. The presented analyses are based on searches performed with the existing 8 TeV dataset. In Section 3 we discuss the expected reach of a generic analysis based on the search for jets and missing hadronic energy, based on Ref. [10]. This is followed in Section 4 by a dedicated search for gluino-induced stop quark production in a final state con-

taining a single lepton, b-tagged jets and missing transverse energy, an extension of the analysis reported in Ref. [11]. The analysis in Section 5 searches for the production of chargino and neutralino particles decaying to W and Z bosons and the lightest neutralinos. This search is based on an analysis described in Ref. [12] with final states including three leptons. In Section 6 we investigate the gain of having extended forward tracking for vector boson fusion processes.

2 Detector layout and simulation

The future LHC and High-Luminosity-LHC (HL-LHC) runs are expected to operate at a center-of-mass energy of $\sqrt{s} \approx 14\,\text{TeV}$ and much higher instantaneous luminosity with respect to the initial LHC design value. Inevitably, there will be a significant increase in the number of pileup events associated with each bunch crossing. The detector upgrades for these future runs are designed to cope with such harsh environment, while improving performance at the same time. The "Phase I upgrade" corresponds to the detector configuration that will be installed in the coming long shutdown of the LHC, planned for 2018/19. The Phase I detector will have to cope with a mean of 50 pileup events and is expected to record a luminosity of $300\,\text{fb}^{-1}$ by the end of 2011, after which a "Phase II upgrade" is planned. Then the detector has to be prepared for facing much harder conditions of around 140 pileup events in the HL-LHC. A minimal configuration assumed in the simulation studies for the Phase II upgrades includes:

- Replacement of electromagnetic endcap calorimeter and retrofitting of the hadronic endcap calorimeter;
- Use of the resolution and transverse size representative of a "shashlik" design for the electromagnetic endcap calorimeter;
- Increase of phi segmentation for the hadronic endcap calorimeter by a factor of four;
- Use of the Phase II tracker in barrel and endcap;
- Extension of muon system to full coverage for $|\eta| < 2.4$.

We refer to this scenario as "Phase II Conf3". In addition, a second scenario is considered, including the following additional features:

- Complete replacement of the endcap;
- Use of the Phase II tracker with extended tracker coverage up to $|\eta| < 4$.

This scenario is referred to as "Phase II Conf4".

As a full trigger table is not available for the Phase II upgrade, all analyses assume triggers similar to the one used in the 8 TeV data taking. While this is unlikely to happen at higher pileup without a major trigger upgrade and it is well possible that the baseline selections will have to be modified in the future, most signal regions are in the tails of distributions that are likely to be triggered without problems.

In this study we investigate the physics reach with these detector configurations. The detector response is simulated using the Delphes 3.0.10 fast simulation program [13], both for signal and background events.

Delphes is able to include pileup from minimum bias collisions that are randomly selected from a file containing inelastic proton-proton interactions produced with PYTHIA6 [14]. These events are randomly distributed along the beam axis (also called z-axis) according to a Gaussian distribution with a width of 0.05 m. When the z-position of a pileup vertex is less than the 0.1 cm from the primary vertex, the pileup interaction is not separated from the additional

vertices, and all particles from both the pileup and primary interactions are included in the object reconstruction. For pileup interactions with a larger z-vertex difference to the primary vertex, the subtraction of charged pileup particles within the tracker volume is applied with an efficiency of unity. The FastJet area method [15] is applied to correct measurements of jets and energy in the calorimeters for the contribution from neutral pileup particles and charged pileup particles outside the tracker acceptance.

About 10 to 100 million events per background process are produced with MADGRAPH5 [16], including up to four extra partons from initial and final state radiation, matched to PYTHIA6 for fragmentation and hadronization. The background cross section is normalized to next-to-leading order (NLO) in the background production process, which is based on the work in preparation for the Snowmass summer study 2013 and discussed in more detail in Refs. [17–19]. While we studied all the major sources of background events, not all background processes with low cross sections that might become relevant at 3000 fb^{-1} are included in these preliminary studies.

The VBF signal is produced with MADGRAPH5. The other signal samples are generated with PYTHIA6 and passed through the Delphes simulation. For PYTHIA6 the tune Z2* [20] is always used. The signal cross sections are calculated at LO for the VBF DM production and to NLO with Prospino2 [21, 22] for the other signal models.

In addition, a few SM processes are produced with a GEANT4 [23] based "full simulation" to validate the Delphes simulation.

3 Search for SUSY in final states with jets and missing hadronic energy

This search targets R-parity conserving SUSY scenarios, where heavy colored particles are produced, relying on the assumption that long decay chains lead to signatures with multiple jets and large missing transverse momentum. Several searches were performed by the CMS Collaboration based on data taken at 7 and 8 TeV [24–26], also exploiting search variables such as α_T [27–29], Razor [30], and M_{T2} [31].

The signal considered in this study is gluino pair production, in which each gluino decays to two jets and the LSP as shown in Fig. 1.

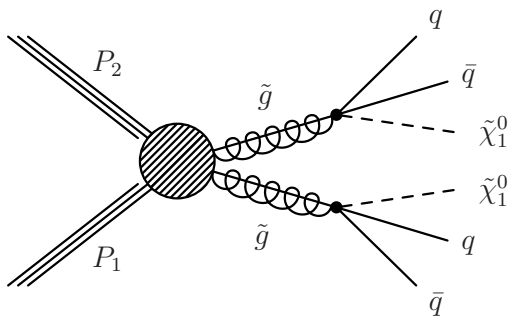

Figure 1: Diagram of gluino-gluino production in which each gluino decays to two jets and the LSP.

The signal is expected to lead to a large amount of hadronic energy $H_{\text{T}} = \sum_{\text{jets}} p_{\text{T}}$ for jets with $p_{\text{T}} > 50\,\text{GeV}$ and $|\eta| < 2.5$, in conjunction with missing hadronic transverse energy which is

defined as $\not{H}_T = |-\sum_{\text{jets}} \vec{p}_T|$ for jets with $p_T > 30\,\text{GeV}$ and $|\eta| < 5$.

The SM background to this SUSY search comes mainly from three processes: $Z(\nu\bar{\nu})$ + jets events, $W(\ell\nu)$ + jets events from W or $t\bar{t}$ + jets, where at least one W boson decays leptonically (ℓ = e, μ, or τ). The $W(\ell\nu)$ + jets events pass the search selection when the e/μ escapes detection or a τ decays hadronically. QCD multijet events also contribute to the background when jet energy mismeasurements or leptonic decays of heavy-flavor hadrons inside jets lead to $\not{H}_T$; however, the QCD background generally becomes negligibly small at high $\not{H}_T$, so it is not considered in this study. The contributions from other SM processes are found to be negligible in previous studies at 8 TeV.

The baseline event selection criteria are taken from the 8 TeV analysis [26]:

- At least three jets with $p_T > 50\,\text{GeV}$ and $|\eta| < 2.5$; jets are reconstructed with the anti-k_t algorithm with the distance parameter $R = 0.5$,
- $H_T > 500\,\text{GeV}$;
- $\not{H}_T > 200\,\text{GeV}$;
- $|\Delta\phi(J_n, \vec{\not{H}}_T)| > 0.5$ rad for $n = 1, 2$ and $|\Delta\phi(J_3, \vec{\not{H}}_T)| > 0.3$ rad, where $\Delta\phi$ is the azimuthal angle difference between the jet axis J_n and the $\vec{\not{H}}_T$ direction for the three highest-p_T jets in the event;
- No isolated muons with $p_T > 10\,\text{GeV}$ and $|\eta| < 2.4$ or electrons with $p_T > 10\,\text{GeV}$ and $|\eta| < 2.5$.

Events passing the baseline selection are considered for the search. The most recent search by CMS with this search strategy [26] divides these events further into several exclusive search regions defined according to the jet multiplicity (n_{jets}), H_T, and $\not{H}_T$. In this projection study, for simplicity, we use several inclusive search regions defined by jet multiplicity, H_T, and $\not{H}_T$. The signal events considered here have four jets at tree level; however, they are often observed to have > 4 jets to due QCD initial- and final-state radiation. The search selection with $n_{\text{jets}} \geq 6$ tends to give a stronger sensitivity compared to the search selection with $n_{\text{jets}} \geq 4$ and $n_{\text{jets}} \geq 5$, as the higher jet multiplicity selection reduces the number of background events more than signal events. We assumed the 30% uncertainty on the background prediction, based on the typical background uncertainty in the recent CMS analysis [26]. The search selection for the $300\,\text{fb}^{-1}$ scenario is listed in the following:

- Search region 1: $n_{\text{jets}} \geq 6$, $H_T > 2100\,\text{GeV}$, and $\not{H}_T > 700\,\text{GeV}$. This search region is sensitive to high gluino mass points.
- Search region 2: $n_{\text{jets}} \geq 6$, $H_T > 1100\,\text{GeV}$, and $\not{H}_T > 600\,\text{GeV}$. This one is sensitive to high LSP masses.
- Search region 3: $n_{\text{jets}} \geq 6$, $H_T > 1600\,\text{GeV}$, and $\not{H}_T > 700\,\text{GeV}$. This search region is used to cover medium gluino and medium LSP mass signal points.
- Search region 4: $n_{\text{jets}} \geq 6$, $H_T > 800\,\text{GeV}$, and $\not{H}_T > 400\,\text{GeV}$. This search region is sensitive to low gluino and low LSP mass signal points.

For the $3000\,\text{fb}^{-1}$ case, the event selection consists the following search regions:

- Search region 1: $n_{\text{jets}} \geq 6$, $H_T > 2500\,\text{GeV}$, and $\not{H}_T > 1000\,\text{GeV}$. This search region is sensitive to high gluino mass points.
- Search region 2: $n_{\text{jets}} \geq 6$, $H_T > 1600\,\text{GeV}$, and $\not{H}_T > 700\,\text{GeV}$. This one is sensitive to high LSP masses.

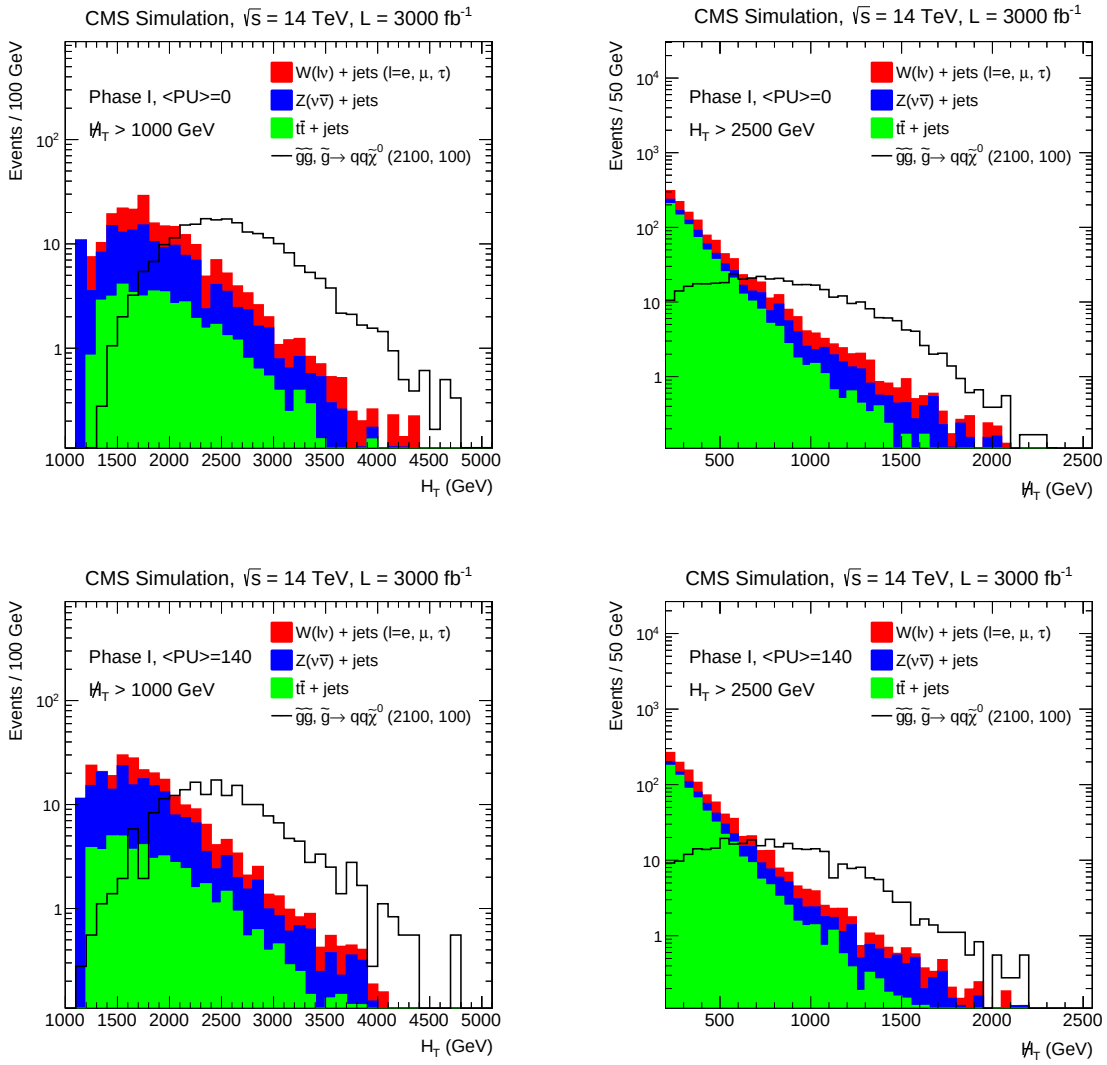

Figure 2: H_T (left) and $\not{H}_T$ (right) distributions for both signal and background for the 14 TeV, 3000 fb^{-1} scenario. Both plots on the top are done with the Phase I detector without pileup interactions, while the bottom plots are done for the same detector configuration, but with 140 pileup interactions. The signal distribution is for the gluino mass and LSP mass of 2100 and 100 GeV, respectively.

- Search region 3: $n_{\text{jets}} \geq 6$, $H_T > 2000$ GeV, and $\not{H}_T > 1000$ GeV. This search region is used to cover medium gluino and medium LSP mass signal points.
- Search region 4: $n_{\text{jets}} \geq 6$, $H_T > 800$ GeV, and $\not{H}_T > 400$ GeV. This search region is sensitive to low gluino and low LSP mass signal points.
- Search region 5: $n_{\text{jets}} \geq 6$, $H_T > 1100$ GeV, and $\not{H}_T > 600$ GeV. This search region is sensitive to low gluino and high LSP mass signal points.

For each signal point, we evaluate the discovery sensitivity for all search regions, of which the one resulting in the best sensitivity is chosen.

The H_T and $\not{H}_T$ distributions for events passing the baseline selection of a SUSY search with jets and $\not{E}_T$ are shown in Fig. 2 for the Phase I detector with mean numbers of pileup interactions,

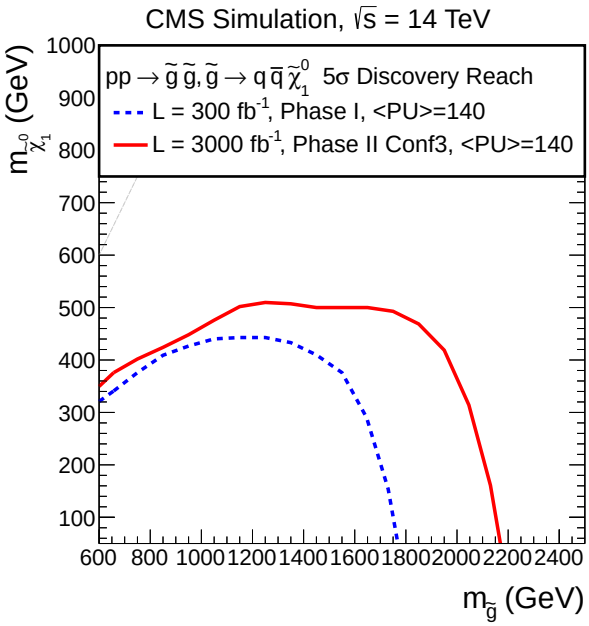

Figure 3: The projected 5σ discovery reaches for pair production of gluinos decaying to four quarks and two LSPs. The blue curve is for $300\,\text{fb}^{-1}$ data with the Phase I detector. The red curve is for $3000\,\text{fb}^{-1}$ with the Phase II Conf3 detector. The result is not very sensitive to different detector and pileup scenarios, therefore only the result for one configuration is shown.

$\langle \text{PU} \rangle = 0$ and 140, for the $3000\,\text{fb}^{-1}$ scenario. The expected signals of gluino-gluino production are also included for illustration purposes.

The H_T and $\not{H}_\text{T}$ distributions with and without pileup interactions agree quite well with each other, indicating that pileup interactions do not have a major impact in the search regions considered here.

The 5σ discovery reach for the $3000\,\text{fb}^{-1}$ and $300\,\text{fb}^{-1}$ scenarios at $\sqrt{s} = 14\,\text{TeV}$ are shown in Fig. 3. Gluino masses up to $\sim$ 2.2 (1.8) TeV and LSP masses up to $\sim$ 500 (400) GeV can be discovered at 14 TeV with an integrated luminosity of 3000 (300) fb^{-1}.

4 Search for gluinos decaying to top quarks and neutralinos in the single lepton final state

Here we present projections on the sensitivity of the search for gluino production, where gluinos decay preferably to third generation quarks and the LSPs, in events with one lepton (electron or muon), large transverse missing energy, and several jets, some of which are identified as originating from b quarks. This analysis is based on a CMS 8 TeV analysis [11] with optimized search regions.

The relevant backgrounds in this search arise from $\text{t}\bar{\text{t}}$ + jets, W/Z + jets, $\text{t}\bar{\text{t}}$ + W/Z, and single-top quark production. As signal we have chosen the topology where a pair of gluinos is produced and each gluino decays to a pair of $\text{t}\bar{\text{t}}$ quarks and a $\tilde{\chi}_1^0$ as shown in Fig. 4.

The final state consists of 4 W bosons, from the decay of the top quarks, leading with high probability to at least one lepton from one of the W decays, and to large values of missing transverse energy.

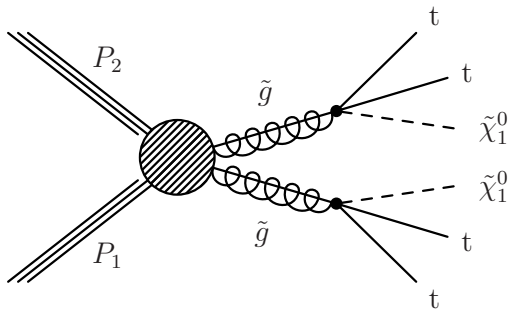

Figure 4: Example of the gluino-induced stop quark production mechanism.

The preselection of events is based on the reconstruction of an isolated lepton (electron or muon) and multiple jets. The selection criteria are as follows:

- An isolated electron (muon) with $p_T > 20\,\text{GeV}$ and $|\eta| < 2.5$ (2.1);
- Veto of additional leptons (electrons or muons) with $p_T > 15\,\text{GeV}$ and $|\eta| < 2.5$;
- At least six jets with $p_T > 40\,\text{GeV}$ and $|\eta| < 2.4$;
- At least one of the jets identified as originating from a b-quark;
- $H_T > 500\,\text{GeV}$, where H_T is the scalar sum of the p_T of all jets in the event with $p_T > 40\,\text{GeV}$ and $|\eta| < 2.4$;
- $S_T^{lep} > 250\,\text{GeV}$, where S_T^{lep} is defined as the scalar sum of the missing transverse energy, $\not{E}_T$, and the p_T of the charged lepton.

After preselection, the sample is dominated by single-lepton $t\bar{t}$ events. This background is reduced by applying a further requirement on the azimuthal angle between the W candidate and the charged lepton. The W candidate transverse momentum is obtained as the vectorial sum of the transverse momentum of the charged lepton, and the missing transverse energy, $\not{E}_T$, which is calculated including all particle flow objects [32]. As discussed in [11], leptons that arise from W decays have a small angle with respect to the W candidate, whereas in SUSY decays the lepton is almost uncorrelated with the $\not{E}_T$ and thus with the resulting W candidate. Therefore, $\Delta\phi(W,\ell) < 1$ is selected as the control region and $\Delta\phi(W,\ell) > 1$ is defined as the signal region for the search. A transfer factor R_{CS} is determined, either from simulation or from data, which is defined as follows:

$$R_{CS} = \frac{N_{signal}}{N_{control}} = \frac{\text{Number of events with } \Delta\phi(W,\ell) > 1}{\text{Number of events with } \Delta\phi(W,\ell) < 1}. \quad (1)$$

Once R_{CS} is known, the number of SM events in the signal region in the data can be estimated from the number of data events in the control region:

$$N_{SM}^{pred}(\Delta\phi(W,\ell) > 1) = R_{CS} \cdot N_{data}(\Delta\phi(W,\ell) < 1). \quad (2)$$

The dominant background in the signal region is di-leptonic $t\bar{t}$. The search is performed in bins of b-tag multiplicity and of S_T^{lep}.

The effect of the increased pileup on the search has been studied in detail for this analysis using the Phase I detector configuration, for two different pileup scenarios, with zero and 140 pileup events. It has been found that the background estimation method will work also under harsh

Table 1: Event yields for the combined electron and muon channels, as expected from simulation for $N_{\text{jet}} \geq 6$ and $N_{\text{b}} \geq 4$ for the Phase II Conf3 detector configuration. For the sample names, V is used to denote W bosons, Z bosons, and photons. The column "R_{CS}" lists the ratio of yields in the signal ($\Delta\phi(\text{W}, \ell) > 1$) region to those in the control ($\Delta\phi(\text{W}, \ell) < 1$) region. The yields for an exemplary signal point are shown for comparison, with the gluino and LSP masses (in GeV) listed in brackets. The uncertainties are statistical only.

$S_{\text{T}}^{\text{lep}}$ region	sample	N_{signal}	N_{control}	R_{CS}
$450 \leq S_{\text{T}}^{\text{lep}} < 550\,\text{GeV}$	$\text{t}\bar{\text{t}}$	16.7±4.5	227.4±19.1	0.073095
	$\text{t}\bar{\text{t}}\text{V}$	0.8±0.2	18.1±4.4	0.047
	single top	0.0±0.0	1.2±0.5	0.038
	V + jets	0.0±0.0	0.0±0.0	0.000
	SM all	17.5±4.5	246.7±19.6	0.071
	signal(2000,300)	6.3±1.0	3.3±0.7	1.909
$550 \leq S_{\text{T}}^{\text{lep}} < 650\,\text{GeV}$	$\text{t}\bar{\text{t}}$	4.4±1.4	76.8±9.8	0.057
	$\text{t}\bar{\text{t}}\text{V}$	0.4±0.1	3.7±0.6	0.109
	single top	0.0±0.0	0.2±0.1	0.211
	V + jets	0.0±0.0	1.6±1.6	0.000
	SM all	4.8±1.4	82.3±9.9	0.059
	signal(2000,300)	5.1±0.9	3.8±0.8	1.360
$650 \leq S_{\text{T}}^{\text{lep}} < 750\,\text{GeV}$	$\text{t}\bar{\text{t}}$	0.8±0.2	29.1±5.1	0.027
	$\text{t}\bar{\text{t}}\text{V}$	0.1±0.0	1.6±0.4	0.055
	single top	0.0±0.0	0.3±0.1	0.000
	V + jets	0.0±0.0	0.0±0.0	0.000
	SM all	0.9±0.2	31.1±5.1	0.028
	signal(2000,300)	7.3±1.1	3.9±0.8	1.885
$S_{\text{T}}^{\text{lep}} \geq 750\,\text{GeV}$	$\text{t}\bar{\text{t}}$	1.5±0.4	15.5±2.8	0.095
	$\text{t}\bar{\text{t}}\text{V}$	0.2±0.1	1.0±0.3	0.162
	single top	0.0±0.0	0.1±0.0	0.050
	V + jets	0.0±0.0	2.5±1.6	0.000
	SM all	1.6±0.4	19.1±3.3	0.086
	signal(2000,300)	31.6±2.2	17.6±1.6	1.803

pileup conditions, and the analysis strategy can stay the same. The search regions in $S_{\text{T}}^{\text{lep}}$ and N_{b} are tighter than in the 8 TeV analysis and defined as follows:

- $S_{\text{T}}^{\text{lep}}$: [450, 550), [550, 650), [650, 750), and $\geq 750\,\text{GeV}$
- N_{b}: =3, $\geq$4

Table 1 shows the event yields expected from simulation for the Phase II Conf3 detector configuration in the signal and control regions for events with $N_{\text{b}} \geq 4$, in different $S_{\text{T}}^{\text{lep}}$ bins. An important ingredient of this analysis is the extended use of data for the estimation of the SM background in the signal region.

The transfer factor R_{CS} has been checked to be roughly independent of the b-jet multiplicity, and is calculated for events with $N_{\text{b}} = 2$. This adaptation comes with the advantage of a much smaller W + jets contamination, when compared to R_{CS} extraction for events with $N_{\text{b}} = 1$ (as done for the 8 TeV analysis), and has the added value of the kinematics being more similar to

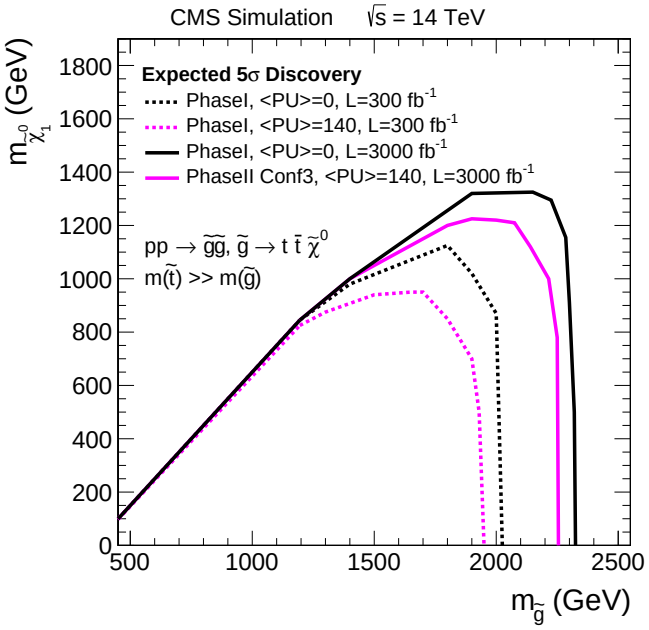

Figure 5: The projected 5σ discovery reach for a simplified model describing gluino production, with each gluino decaying to a $t\bar{t}$ pair and an LSP, for $300\,\text{fb}^{-1}$ (dashed curves) and $3000\,\text{fb}^{-1}$ (solid curves). The discovery reach is shown for $\langle\text{PU}\rangle = 0$ (black) and $\langle\text{PU}\rangle = 140$ (magenda).

those of events with larger b-tag multiplicities. To correct for any residual dependencies, we assign correction factors (k_{CS}) from simulation. The uncertainty of these factors is of the order of 30% and mainly caused by the limited statistics of the Delphes samples.

Figure 5 illustrates the 5σ discovery potential for a center-of-mass energy $\sqrt{s} = 14\,\text{TeV}$ and an integrated luminosity of $300\,\text{fb}^{-1}$ and $3000\,\text{fb}^{-1}$. The discovery range of gluinos can be enhanced by 300 GeV for from $300\,\text{fb}^{-1}$ to $3000\,\text{fb}^{-1}$ up to 2.2 TeV, for a χ_1^0 with mass of up to 1.2 TeV. The mass reach is mitigated due to pileup by about 100 GeV.

5 EWKino search with final states including three leptons and missing transverse energy

Searches for the direct electroweak production of SUSY particles are challenging at the LHC due to its low production cross section and low hadronic activities in the event. The mass reach for weakly-produced SUSY particles is generally weaker than that for the strongly-produced SUSY particles; however, the large integrated luminosity expected from HL-LHC would allow extending our sensitivity to weakly-produced SUSY particles significantly. In this section, future sensitivities of the analysis designed to discover the direct production of charginos ($\chi_1^{\pm}$) and neutralinos (χ_2^0), that decay via a W and Z boson, are presented based on a CMS 8 TeV search [12]. Depending on the actual flavor structure of the χ_2^0, the concurrent χ_2^0 decay mode can also be $\chi_2^0 \to H\chi_1^0$. However, as a baseline for this study we assume the simplified model presented in Fig. 6 with $\text{Br}(\chi_2^0 \to Z\chi_1^0) = 100\%$. In order to reduce the background as efficiently as possible, we concentrate on the decays where both bosons decay leptonically, leading to a final state with three leptons.

We select muons and electrons with a transverse momentum of at least $p_{\text{T}} > 10\,\text{GeV}$. The leading lepton is required to have $p_{\text{T}} > 20\,\text{GeV}$, corresponding to the trigger thresholds in

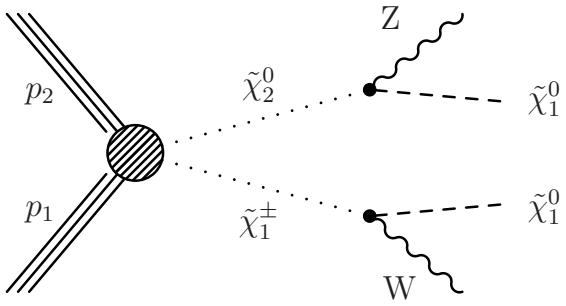

Figure 6: Feynman diagram for direct chargino-neutralino production. The chargino decays via a W boson into the LSP, and the neutralino decays via a Z boson into the LSP. We concentrate on scenarios where both leptons decay leptonically.

2012. Additionally, the leptons are required to be within $|\eta| < 2.4$. We require the presence of a pair of leptons with same flavor and opposite charge (OSSF), which forms most likely the Z boson. If more than one OSSF pair is found, the pair closest to the Z-boson mass is chosen, and the remaining lepton is assigned to the W decay. The OSSF pair invariant mass has to be close to the Z boson mass (between 75 GeV and 105 GeV). The two LSPs in the final state escape the detector without any interaction, leading to missing transverse energy in the detector. A large number of pileup events results in worse $\not{E}_T$ resolution and thus degrades the sensitivity in this search. These selection requirements are inherited from the CMS 8 TeV search and not optimized to a 14 TeV search at high pileup.

Several standard model processes lead to a similar signature of three leptons and high $\not{E}_T$ in the final state, mainly WZ production, followed by $t\bar{t}$ background, rare processes, and single-boson production. All four backgrounds are discussed in detail below.

The WZ production results in almost the same signature, but the source of $\not{E}_T$ for this background is the decay of the W boson. Therefore, we introduce the variable M_T defined as:

$$M_T = \sqrt{2\not{E}_T p_T^{\ell_3} \left[1 - \cos\left(\Delta\phi(\ell_3, \not{E}_T)\right)\right]} \tag{3}$$

where $p_T^{\ell_3}$ is the lepton assigned to the W. For WZ background the variable M_T should have a sharp kink at the W boson mass of about 80 GeV. It has been shown that this variable has a good discrimination power between signal and WZ background. In the 8 TeV CMS search [12], the prediction of this background relies mostly on simulation. A comparison between the Delphes simulation and the full detector simulation shows good agreement, assuring that also a prediction with Delphes will lead to similar results as the prediction for the 8 TeV search with full simulation.

The second most important background is $t\bar{t}$ production, where two leptons come from W decay and one lepton produced in a jet passes the lepton isolation criteria and will be identified as isolated lepton. Jets containing a b quark have a higher probability for this. Backgrounds from $t\bar{t}$ are suppressed by vetoing events with b-tagged jets.

Several rare processes can have three leptons in the final state, including triple boson production, $t\bar{t}$ + boson production and Higgs-boson production. These backgrounds have one thing in common, the small cross section. Since some of these backgrounds could have intrinsic $\not{E}_T$ in the final state, they become important at high $\not{E}_T$ and high M_T .

Single-boson backgrounds have at most two prompt leptons in the final state. But here again additional leptons might escape a jet, or a hadron could be misidentified as lepton. This kind

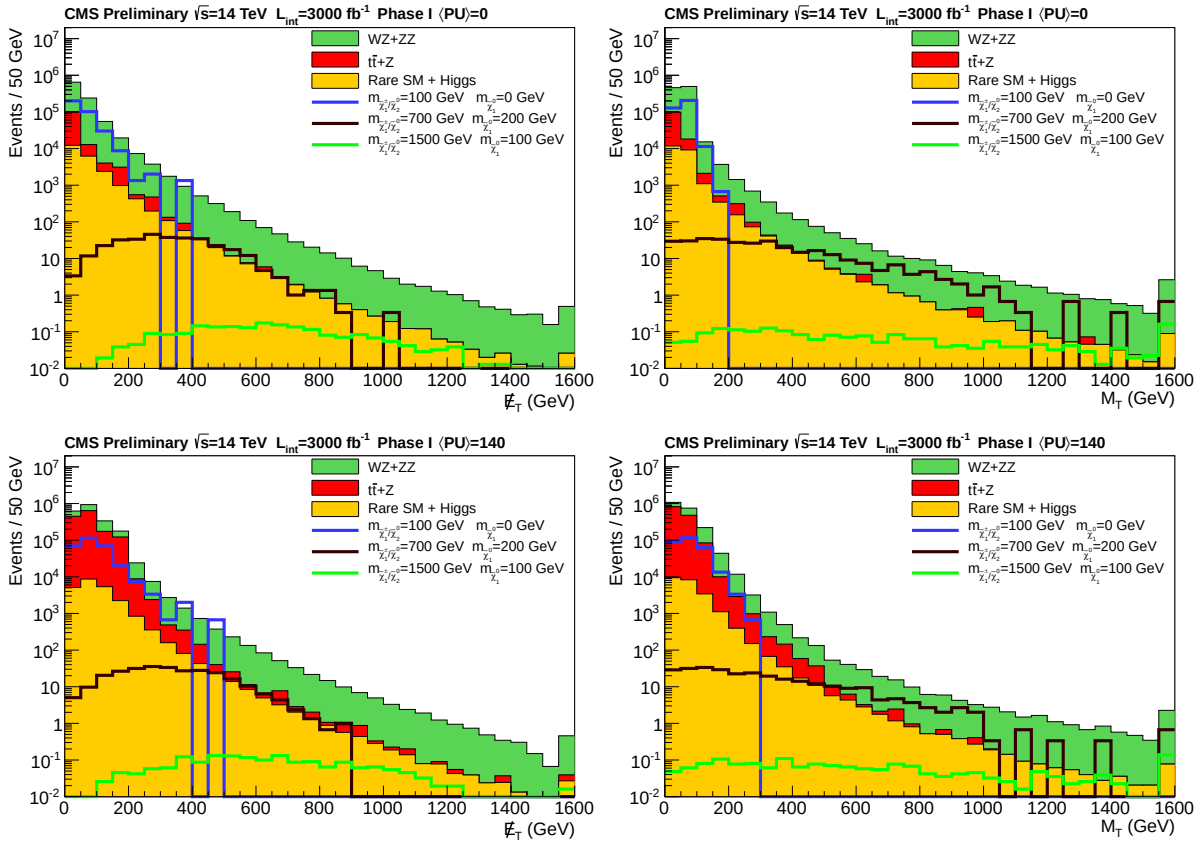

Figure 7: The $\not{E}_T$ (left) and the M_T distribution (right) for event with 3 leptons and a b-veto for the Phase I detector with zero pileup (top) and 140 pileup events (bottom). In addition to the SM predictions some possible SUSY benchmark scenarios are included.

of background has no intrinsic $\not{E}_T$ and is therefore suppressed by requiring large $\not{E}_T$.

In Fig. 7 the $\not{E}_T$ and M_T distributions are shown for the same detector configuration (Phase I) with zero and 140 pileup events. The $t\bar{t}$ and Drell-Yan contribution increases for the scenarios with a mean pileup of 140 in the regions of lower $\not{E}_T$ and M_T . This is caused by a higher fake rate in high-pileup scenarios, and is expected to be reduced in future analyses by optimized selection requirements, e.g. a higher lepton p_T.

We choose several signal regions defined by an asymmetric binning in M_T and $\not{E}_T$, due to the correlation between them. The standard model predictions for three different scenarios are listed in Table 2. At intermediate M_T and $\not{E}_T$ values we observe the largest pileup dependence.

As shown in Fig. 8, with 300 fb^{-1} we are sensitive to $\chi_1^\pm$ and χ_2^0 masses up to 500 GeV for χ_1^0 masses up to $\sim$ 150 GeV in simplified model describing chargino-neutralino production with 100% branching fraction to a W and a Z boson and LSPs. This mass range can be extended to $\chi_1^\pm$ and χ_2^0 masses up to 700 GeV and χ_1^0 masses up to $\sim$ 200 GeV for a luminosity of 3000 fb^{-1}. As a $\chi_2^0 \to Z\chi_1^0$ branching ratio of 100% may be an unrealistic scenario, we show here for illustration the result for a branching ratio of 50%.

Table 2: Standard model background predictions for the different scenarios at 3000 fb^{-1}.

Selection in GeV		Phase I $\langle$PU$\rangle$=0 yield $\pm$ uncert.	Phase I $\langle$PU$\rangle$=140 yield $\pm$ uncert.	Phase II Conf3 $\langle$PU$\rangle$=140 yield $\pm$ uncert.
$0 < M_T < 120$	$0 < \not{E}_T < 60$	$(7.3 \pm 0.7) \times 10^5$	$(8.0 \pm 1.2) \times 10^5$	$(9.3 \pm 1.2) \times 10^5$
$0 < M_T < 120$	$60 < \not{E}_T < 120$	$(1.8 \pm 0.2) \times 10^5$	$(8.4 \pm 1.2) \times 10^5$	$(9.3 \pm 1.1) \times 10^5$
$0 < M_T < 120$	$120 < \not{E}_T < \infty$	$(5.6 \pm 0.8) \times 10^4$	$(3.3 \pm 0.7) \times 10^5$	$(3.3 \pm 0.7) \times 10^5$
$120 < M_T < 200$	$0 < \not{E}_T < 120$	$(7.9 \pm 0.8) \times 10^3$	$(7.7 \pm 0.7) \times 10^4$	$(8.2 \pm 0.7) \times 10^4$
$120 < M_T < 200$	$120 < \not{E}_T < 200$	$(1.2 \pm 0.2) \times 10^3$	$(4.0 \pm 0.7) \times 10^4$	$(4.3 \pm 0.7) \times 10^4$
$120 < M_T < 200$	$200 < \not{E}_T < \infty$	359 ± 84	$(5.7 \pm 2.3) \times 10^3$	$(4.8 \pm 2.1) \times 10^3$
$200 < M_T < 400$	$0 < \not{E}_T < 200$	$(2.3 \pm 0.2) \times 10^3$	$(1.5 \pm 0.2) \times 10^4$	$(1.5 \pm 0.2) \times 10^4$
$200 < M_T < 400$	$200 < \not{E}_T < 400$	303 ± 52	$(1.6 \pm 0.5) \times 10^3$	$(1.4 \pm 0.5) \times 10^3$
$200 < M_T < 400$	$400 < \not{E}_T < \infty$	24 ± 4	69 ± 35	39 ± 12
$400 < M_T < 700$	$0 < \not{E}_T < 300$	249 ± 24	395 ± 58	390 ± 42
$400 < M_T < 700$	$300 < \not{E}_T < 700$	67 ± 13	95 ± 19	100 ± 24
$400 < M_T < 700$	$700 < \not{E}_T < \infty$	1.1 ± 0.4	1.3 ± 0.5	1.4 ± 0.4
$700 < M_T < \infty$	$0 < \not{E}_T < 400$	30 ± 3	27 ± 3	27 ± 3
$700 < M_T < \infty$	$400 < \not{E}_T < 900$	32 ± 5	31 ± 5	30 ± 5
$700 < M_T < \infty$	$900 < \not{E}_T < \infty$	1.4 ± 0.4	1.5 ± 0.5	1.2 ± 0.4

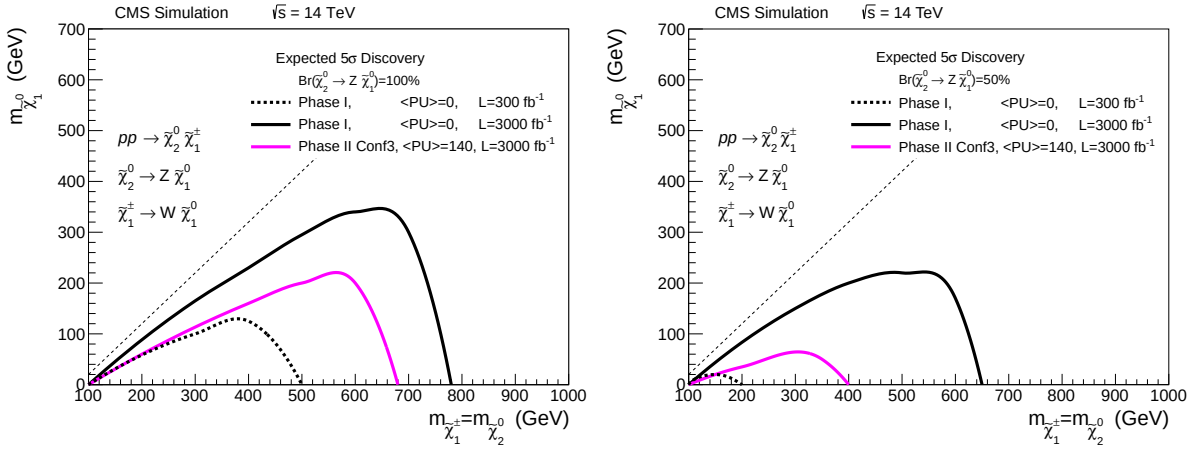

Figure 8: 5σ discovery reach for the simplified model describing the direct production of charginos and neutralinos, that decay to 100% via a W and Z boson for 3000 fb^{-1} (left), for a mean of 140 pileup events with the upgraded Phase II detector (solid magenta line), and also for zero pileup with the Phase I detector (black solid line). Results for 300 fb^{-1} with zero pileup are displayed as dashed lines. A $\chi_2^0 \to Z\chi_1^0$ branching ratio of 100% may be not realistic. To illustrate the migration of the discovery reach due to a smaller branching ratio, we show here for illustration the result for a branching ratio of 50% as well (right).

6 Dark matter search in vector boson fusion processes

Vector boson fusion processes [5, 6] at the LHC provide a unique opportunity to search for new physics with electroweak couplings [33–35]. In this section, studies on detecting supersymmetric dark matter produced directly at HL-LHC in VBF processes are reported. Here we consider a model in which the lightest neutralino $\tilde{\chi}_1^0$ is the LSP, a viable candidate of DM. The $\tilde{\chi}_1^0$ and $\tilde{\chi}_1^\pm$ are mainly Wino and nearly mass-degenerate, so that both $\tilde{\chi}_1^0$ and $\tilde{\chi}_1^\pm$ are invisible in the detector. These $\tilde{\chi}_1^0$ or $\tilde{\chi}_1^\pm$ could be produced directly at the LHC through VBF processes as shown in

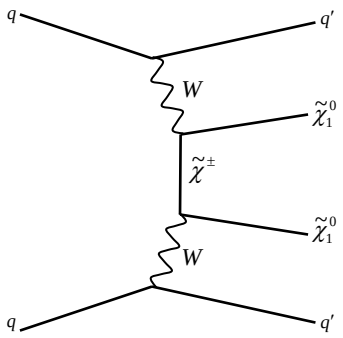

Figure 9: Diagram for $\tilde{\chi}_1^0\tilde{\chi}_1^0$ production via VBF process.

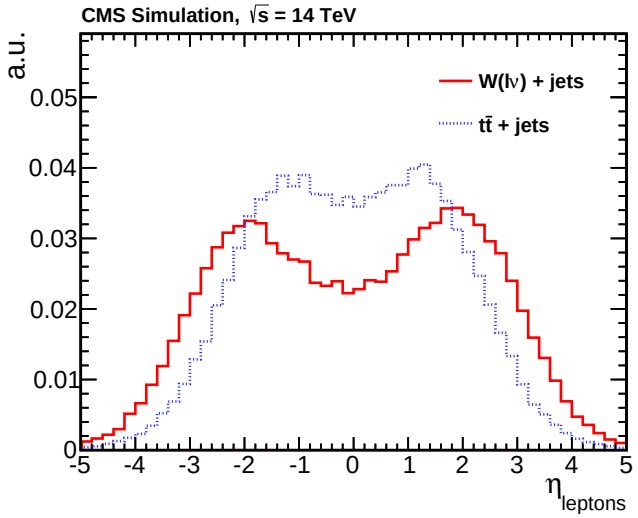

Figure 10: The lepton η distribution in W + jets and $t\bar{t}$ events after the loose VBF selection used in [33].

Fig. 9. The signal is characterized by the presence of two jets with large dijet invariant mass in the forward region in opposite hemispheres and a large $\not{E}_T$. This search is very challenging due to the small production cross section of the signal; however, the HL-LHC data may allow us to discover it [34].

The background samples considered are the W and Z + jets production samples with jets arising from QCD interactions and the VBF production of W and Z. These processes constitute the major background in this search. The $t\bar{t}$ production is also considered. The signal model considered is the pure Wino dark matter scenario with $m_{\tilde{\chi}_1^0} = 112$, 200, and 500 GeV.

The Phase II Conf4 option of the upgraded detector, with the extended tracker coverage up to $|\eta| < 4$, can benefit this search mainly in the following two ways:

- The improved lepton acceptance reduces W and $t\bar{t}$ backgrounds, major background sources in this search, through the lepton vetos.
- The improved pileup mitigation (pileup charged hadron subtraction) in the forward region based on tracking is expected to improve the VBF jet tagging and $\not{E}_T$ resolution, two main aspects in this search.

For the first point, one can see the benefit from the lepton η distribution, which is shown in

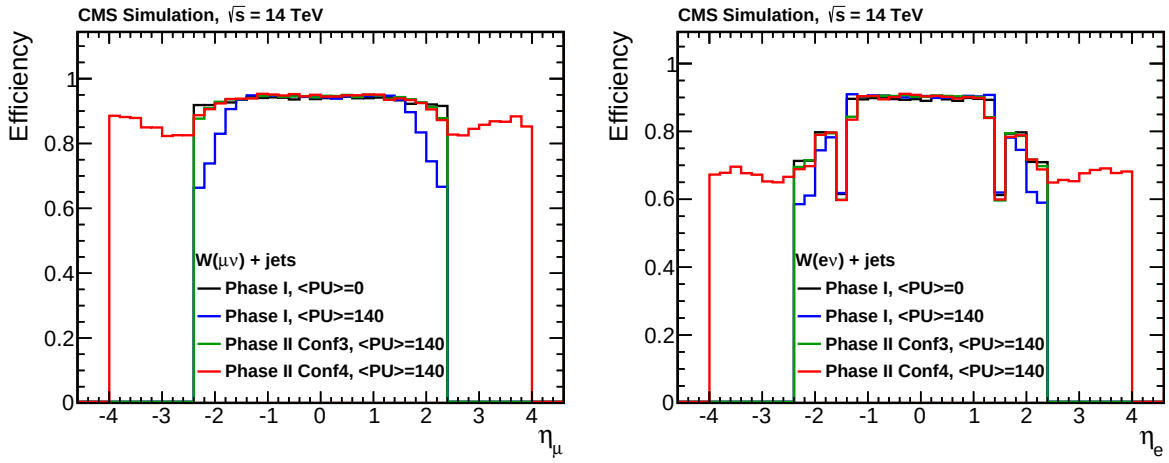

Figure 11: Muon (left) and electron (right) selection efficiencies as a function of η. The efficiencies are determined for muons and electrons with $p_T > 5\,\text{GeV}$ in $W(\ell\nu)$ + jets events.

Fig. 10. A significant amount of leptons fall outside the current geometrical acceptance of $|\eta| < 2.5$. The lepton efficiencies in the Delphes simulation, which are verified against the CMS full simulation [36], are shown as functions of η in Fig. 11. The lepton selection efficiency is crucial in order to achieve high efficiency for lepton vetoes to reduce W and $t\bar{t}$ backgrounds. The effect of the increased lepton acceptance in η can be clearly observed in Fig. 11.

Figure 12 shows jet η distributions for jets with $p_T > 30\,\text{GeV}$ in $W(\ell\nu)$ + jets events. The pileup jets outside the tracking coverage are clearly visible in Fig. 12 in the forward region outside the tracking coverage for 140 pileup scenarios, where charged hadrons from pileup pp interactions cannot be subtracted on a particle-by-particle basis. In order to reduce the large contributions from pileup jets in the forward region, a higher jet p_T threshold cuts are applied for the 140 pileup scenarios for VBF jets selection. Although the detailed structure is still under investigation, the distribution for the Phase II Conf4 detector shows a clear indication that the extended tracker coverage can mitigate pileup jets substantially up to $|\eta| \sim 4$.

Figure 13 shows the $\not{H}_T$ and M_{jj} distributions for $W(\ell\nu)$ + jets events, where $\not{H}_T$ is the magnitude of the vector sum of all the reconstructed leptons, photons, and jets with $p_T > 30\,\text{GeV}$ and $|\eta| < 5$. The pileup jet contributions are clearly visible in these distributions. The $\not{H}_T$ distributions show a factor of ~ 10 more events at $\not{H}_T > 200\,\text{GeV}$ in the 140 pileup scenario with the Phase I and II Conf3 detectors compared to the zero pileup scenario, while the Phase II Conf4 detector shows only a factor of < 2 increase. Similarly, the M_{jj} distribution shows a significant reduction at $M_{jj} > 1500\,\text{GeV}$ with the Phase II Conf4 detector compared to the Phase I and Phase II Conf3 detectors.

The baseline event selection adopted for this search is as follows:

- VBF selection:
  - $\not{H}_T > 50\,\text{GeV}$;
  - $p_T^{jet1,2} > 50\,\text{GeV}$;
  - $|\eta^{jet1,2}| < 5$;
  - $|\eta^{jet1} - \eta^{jet2}| > 4.2$;
  - $\eta^{jet1} \cdot \eta^{jet2} < 0$;
- $p_T^{jet1} > 50\,\text{GeV}$ (200 GeV for 140 pileup scenarios);

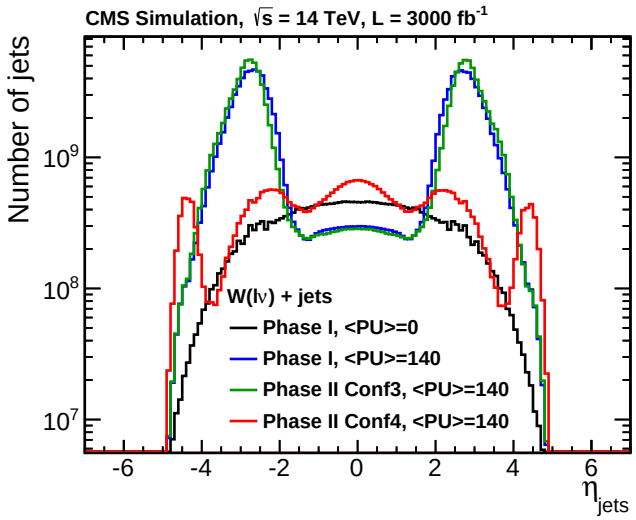

Figure 12: Pseudorapidity distributions for jets with $p_{\mathrm{T}} > 30\,\mathrm{GeV}$ for various pileup and detector configurations in $\mathrm{W}(\ell\nu)$ + jets events.

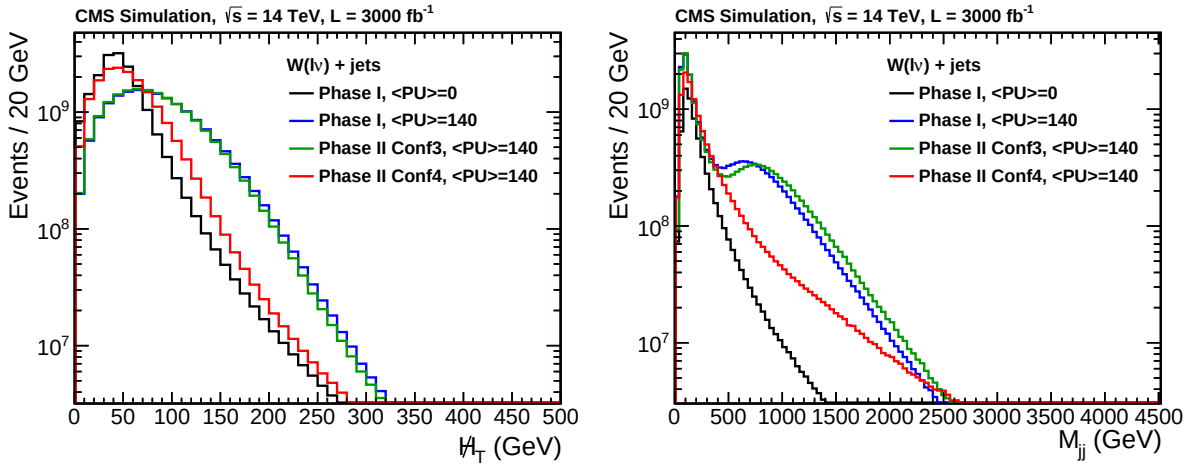

Figure 13: Comparison of $\not{H}_{\mathrm{T}}$ and M_{jj} distributions in $\mathrm{W}(\ell\nu)$ + jets samples from different detectors with different pileup scenarios. All $\mathrm{W}(\ell\nu)$ + jets events without any event selection are shown for $\not{H}_{\mathrm{T}}$ distributions and $\mathrm{W}(\ell\nu)$ + jets events with at least two jets with $p_{\mathrm{T}} > 30\,\mathrm{GeV}$ are shown for M_{jj} distributions.

- $p_{\mathrm{T}}^{\mathrm{jet2}} > 50\,\mathrm{GeV}$ (100 GeV for 140 pileup scenarios);
- $M_{\mathrm{jj}} > 1500\,\mathrm{GeV}$;
- Veto a third jet with $p_{\mathrm{T}}^{\mathrm{jet3}} > 30\,\mathrm{GeV}$ lying between the leading two jets;
- Veto a b-tagged jet;
- Veto a lepton (electron, muon, and tau);
- $\not{H}_{\mathrm{T}} > 200\,\mathrm{GeV}$.

After these baseline event selection requirements, the Phase II Conf4 detector shows much reduced backgrounds compared to other detector configurations studied, while reducing the signal efficiency only by about 10%, with the same pileup condition of $\langle \mathrm{PU} \rangle = 140$. The $\mathrm{Z}(\nu\bar{\nu})$ + jets background reduces by a factor of about 2 with the Phase II Conf4 detector compared to

the Phase I and Phase II Conf3 detectors, which arises from the improved M_{jj} reconstruction and $\not{H}_T$ resolution. The $W(\ell\nu)$ + jets background reduces by a factor of about 5 with the Phase II Conf4 detector. This further reduction in $W(\ell\nu)$ + jets events compared to the reduction in $Z(\nu\bar{\nu})$ + jets events is attributed to the increased lepton acceptance to improve the lepton vetos. In fact, the muon veto reduces the $W(\mu\nu)$ + jets background to 31% with Phase II Conf3 detector, while it reduces to 9% with the Phase II Conf4 detector. Further studies for achieving the similar level of performance for the electrons and tau leptons as well as for understanding the projected systematic uncertainties are necessary to present the discovery potential of this search at HL-LHC.

7 Summary and Conclusion

We have investigated the discovery reach for several SUSY searches, which are interpreted within simplified models.

For a SUSY search in a final state with jets and missing hadronic energy, interpreted in a simplified model of gluinos decaying to squarks, the 5σ significance is enhanced for gluino masses up to $\sim$ 2.2 TeV and LSP masses up to $\sim$ 500 GeV at 14 TeV with an integrated luminosity of 3000 fb^{-1}, which is an improvement of about 400 GeV in gluino masses compared to the reach at 300 fb^{-1}.

A similar improvement is found for a search in final states with a single lepton, b-tagged jets and missing transverse energy which is interpreted in a benchmark model with pair-production of gluinos, each of which subsequently decaying to $t\bar{t}$ and χ_1^0. In this model, gluinos with a mass smaller than about 2.2 TeV for neutralino masses below about 1.2 TeV can be discovered with 3000 fb^{-1}, yielding a gain of 300 GeV compared to 300 fb^{-1}.

A model describing direct production of charginos ($\chi_1^\pm$) and neutralinos (χ_2^0), that decay with a branching fraction of 100% via a W and Z boson, has also been investigated. With 3000 fb^{-1} we are able to discover $\chi_1^\pm$ and χ_2^0 masses up to 700 GeV for χ_1^0 masses up to $\sim$ 200 GeV. The improvement in the mass reach for $\chi_1^\pm$ and χ_2^0 is about 200–300 GeV compared to the projected reach at 300 fb^{-1}.

SUSY analyses with zero [24–31] or one leptons [11, 37] in the final state tend to be dominated by standard model backgrounds where one charged lepton from a leptonic W decay is not found. We investigated the impact of an extended tracking detector up to a pseudorapidity of $|\eta| < 4$ for the case of $W \to \mu\nu$, and find that the lost lepton background is reduced by a factor three. Further studies on electrons and taus are needed before this level of improvement can be propagated into a mass reach via an actual analysis.

In general, the high-luminosity LHC with an average of about 140 pileup events imposes challenging conditions on jet reconstruction, especially in the forward region beyond $|\eta|$ of about 2. The effect of high pileup on the jet multiplicities at large pseudorapidities can be mitigated significantly by the extended tracker. In addition, the charged-particle subtraction leads to a better jet energy reconstruction over the whole range covered by the tracker, which improves the pileup rejection in the forward region significantly. This is of crucial importance for vector boson fusion processes, but also improves the measurement of the hadronic energy in the event and the missing energy resolution, and will therefore improve most SUSY analyses. The sensitivity for SUSY production in vector boson fusion processes will be evaluated in more detail in future analyses.

References

[1] N. Sakai, "Naturalness in Supersymmetric GUTS", *Z. Phys. C* **11** (1981) 153, doi:10.1007/BF01573998.

[2] S. Dimopoulos and G. Giudice, "Naturalness constraints in supersymmetric theories with nonuniversal soft terms", *Phys. Lett. B* **357** (1995) 573, doi:10.1016/0370-2693(95)00961-J, arXiv:hep-ph/9507282.

[3] Planck Collaboration, "Planck 2013 results. XVI. Cosmological parameters", arXiv:1303.5076.

[4] WMAP Collaboration, "Nine-Year Wilkinson Microwave Anisotropy Probe (WMAP) Observations: Cosmological Parameter Results", arXiv:1212.5226.

[5] R. Cahn and S. Dawson, "Production of Very Massive Higgs Bosons", *Phys. Lett. B* **136** (1984) 196, doi:10.1016/0370-2693(84)91180-8.

[6] J. Bjorken, "Rapidity gaps and jets as a new physics signature in very high-energy hadron hadron collisions", *Phys. Rev. D* **47** (1993) 101, doi:10.1103/PhysRevD.47.101.

[7] N. Arkani-Hamed et al., "MARMOSET: The Path from LHC Data to the New Standard Model via On-Shell Effective Theories", arXiv:hep-ph/0703088.

[8] J. Alwall, P. C. Schuster, and N. Toro, "Simplified models for a first characterization of new physics at the LHC", *Phys. Rev. D* **79** (Apr, 2009) 075020, doi:10.1103/PhysRevD.79.075020.

[9] J. Alwall, P. Schuster, and N. Toro, "Simplified Models for a First Characterization of New Physics at the LHC", *Phys. Rev. D* **79** (2009) 075020, doi:10.1103/PhysRevD.79.075020, arXiv:0810.3921.

[10] CMS Collaboration, "Search for New Physics in the Multijets and Missing Momentum Final State in Proton-Proton Collisions at 8 TeV", CMS Physics Analysis Summary CMS-PAS-SUS-13-012, (2013).

[11] CMS Collaboration, "Search for supersymmetry in pp collisions at $\sqrt{s} = 8$ TeV in events with a single lepton, large jet multiplicity, and multiple b-jets", CMS Physics Analysis Summary CMS-PAS-SUS-13-007, (2013).

[12] CMS Collaboration, "Search for electroweak production of charginos, neutralinos, and sleptons using leptonic final states in pp collisions at 8 TeV", CMS Physics Analysis Summary CMS-PAS-SUS-13-006, (2013).

[13] J. de Favereau et al., "DELPHES 3, A modular framework for fast simulation of a generic collider experiment", arXiv:1307.6346.

[14] T. Sjostrand, S. Mrenna, and P. Z. Skands, "PYTHIA 6.4 Physics and Manual", *JHEP* **0605** (2006) 026, doi:10.1088/1126-6708/2006/05/026, arXiv:hep-ph/0603175.

[15] M. Cacciari and G. P. Salam, "Pileup subtraction using jet areas", *Phys. Lett. B* **659** (2008) 119, doi:10.1016/j.physletb.2007.09.077, arXiv:0707.1378.

[16] J. Alwall et al., "MadGraph 5 : Going Beyond", *JHEP* **1106** (2011) 128, doi:10.1007/JHEP06(2011)128, arXiv:1106.0522.

[17] J. Anderson et al., "Snowmass Energy Frontier Simulations", arXiv:1309.1057.

[18] A. Avetisyan et al., "Methods and Results for Standard Model Event Generation at $\sqrt{s}$ = 14 TeV, 33 TeV and 100 TeV Proton Colliders (A Snowmass Whitepaper)", arXiv:1308.1636.

[19] A. Avetisyan et al., "Snowmass Energy Frontier Simulations using the Open Science Grid (A Snowmass 2013 whitepaper)", arXiv:1308.0843.

[20] R. Field, "Early LHC underlying event data - findings and surprises", (2010). arXiv:1010.3558.

[21] W. Beenakker, R. Hopker, M. Spira, and P. Zerwas, "Squark and gluino production at hadron colliders", *Nucl. Phys. B* **492** (1997) 51, doi:10.1016/S0550-3213(97)80027-2, arXiv:hep-ph/9610490.

[22] W. Beenakker et al., "The Production of charginos / neutralinos and sleptons at hadron colliders", *Phys. Rev. Lett.* **83** (1999) 3780, doi:10.1103/PhysRevLett.83.3780, arXiv:hep-ph/9906298.

[23] GEANT4 Collaboration, "GEANT4: A simulation toolkit", *Nucl. Instrum. Meth. A* **506** (2003) 250, doi:10.1016/S0168-9002(03)01368-8.

[24] CMS Collaboration, "Search for New Physics with Jets and Missing Transverse Momentum in pp collisions at $\sqrt{s} = 7$ TeV", *JHEP* **08** (2011) 155, doi:10.1007/JHEP08(2011)155, arXiv:1106.4503.

[25] CMS Collaboration, "Search for Supersymmetry at the LHC in Events with Jets and Missing Transverse Energy", *Phys. Rev. Lett.* **109** (2012) 171803, doi:10.1103/PhysRevLett.109.171803, arXiv:1207.1898.

[26] CMS Collaboration, "Search for New Physics in the Multijets and Missing Momentum Final State in Proton-Proton Collisions at $\sqrt{s} = 8$ TeV", CMS Physics Analysis Summary CMS-PAS-SUS-13-012, (2013).

[27] CMS Collaboration, "Search for Supersymmetry in pp Collisions at 7 TeV in Events with Jets and Missing Transverse Energy", *Phys. Lett. B* **698** (2011) 196, doi:10.1016/j.physletb.2011.03.021, arXiv:1101.1628.

[28] CMS Collaboration, "Search for Supersymmetry at the LHC in Events with Jets and Missing Transverse Energy", *Phys. Rev. Lett.* **107** (2011) 221804, doi:10.1103/PhysRevLett.107.221804, arXiv:1109.2352.

[29] CMS Collaboration, "Search for supersymmetry in final states with missing transverse energy and 0, 1, 2, or at least 3 b-quark jets in 7 TeV pp collisions using the variable α_T", *JHEP* **1301** (2013) 077, doi:10.1007/JHEP01(2013)077, arXiv:1210.8115.

[30] CMS Collaboration, "Inclusive search for squarks and gluinos in pp collisions at $\sqrt{s} = 7$ TeV", *Phys. Rev. D* **85** (2012) 012004, doi:10.1103/PhysRevD.85.012004, arXiv:1107.1279.

[31] CMS Collaboration, "Search for supersymmetry in hadronic final states using M_{T2} in pp collisions at $\sqrt{s} = 7$ TeV", *JHEP* **1210** (2012) 018, doi:10.1007/JHEP10(2012)018, arXiv:1207.1798.

[32] CMS Collaboration, "Particle-Flow Event Reconstruction in CMS and Performance for Jets, Taus, and $E_{\mathrm{T}}^{\mathrm{miss}}$", CMS Physics Analysis Summary CMS-PAS-PFT-09-001, (2009).

[33] B. Dutta et al., "Vector Boson Fusion Processes as a Probe of Supersymmetric Electroweak Sectors at the LHC", *Phys. Rev. D* **87** (2013) 035029, doi:10.1103/PhysRevD.87.035029, arXiv:1210.0964.

[34] A. G. Delannoy, B. Dutta, A. Gurrola, W. Johns, and T. Kamon et al., "Probing Dark Matter at the LHC using Vector Boson Fusion Processes", *Phys. Rev. Lett.* **111** (2013) 061801, doi:10.1103/PhysRevLett.111.061801, arXiv:1304.7779.

[35] CMS Collaboration, "Search for an Invisible Higgs Boson", CMS Physics Analysis Summary CMS-PAS-HIG-13-013, (2013).

[36] CMS Collaboration, "Studies of the performances of the $H \to ZZ^* \to 4\mu$ analysis with the CMS Phase II detector upgrade", CMS Physics Analysis Summary CMS-PAS-FTR-13-003, (2013).

[37] CMS Collaboration, "Search for top-squark pair production in the single-lepton final state in pp collisions at $\sqrt{s} = 8$ TeV", arXiv:1308.1586. Submitted to EPJC.